# Ultralight Supertetrahedral Aluminum: Stability at Various Temperatures

Iliya V. Getmanskii,[a] Vitaliy V. Koval,[a] Nikolay V. Tkachenko,[b]
Stanislav A. Zaitsev,[a] Alexander I. Boldyrev,[b,*] Ruslan M. Minyaev[a,*]

[a]Institute of Physical and Organic Chemistry, Southern Federal University,
Rostov-on-Don 344090, Russian Federation
[b]Department of Chemistry and Biochemistry, Utah State University,
Logan, Utah 84322, United States

KEYWORDS: computer modeling of melting, metallic chemical bond, multicenter chemical bond, solid state calculations, supertetrahedral aluminum

**ABSTRACT:** *Ab initio* molecular dynamics simulations of the structural stability of the allotropic supertetrahedral ultra-light form of aluminum at different temperatures have shown that supertetrahedral aluminum remains structurally stable up to the temperature of 200 K. When being heated to 225 K, supertetrahedral aluminum melts, followed by a liquid to solid phase transition and formation of the face-centered cubic (fcc) structure. The transformation of supertetrahedral aluminum into fcc aluminum is accompanied by an energy release of 4260 kJ/kg. Taking into account its stability at temperatures below 200K, supertetrahedral aluminum would not float in water because water is solid at this temperature, but it would float in liquid nitrogen.

## I. INTRODUCTION

In recent years, computational modeling of the structures and chemical behavior of two- and three-dimensional molecular systems with non-standard combinations of atoms and crystal lattices became an efficient, widely adopted strategy for molecular design of new materials exhibiting unusual physical and mechanical properties. [1-13] Burdett and Lee first proposed replacing atomic lattice sites of a crystal with properly selected structurally matched polyatomic fragments and succeeded in constructing a supertetrahedral clone of a diamond lattice with a carbon tetrahedra instead of carbon atoms.[14] Subsequently, this idea was taken up by Johnston and Hoffmann, who designed the stable supercubane[15] and gained further development in the studies of various novel crystal structures.[11,16,17] This approach appeared to be particularly fruitful in the design of the crystal forms of compounds with non-carbon atoms. We have previously predicted stability and computationally investigated electronic and spatial structures of new allotropic forms of supertetrahedral boron.[18] The logic of the use of a tetrahedral $B_4H_4$ fragment as a structural unit is based on its kinetic stability. Because of electron deficiency of a boron atom this structure does not correspond to the global minimum, but belongs to a local minimum[18] and remains metastable upon substitution of hydrogens by heavy atomic groups. In contrast to tetraborane $B_4H_4$,

alumotetrahedrane $Al_4H_4$ corresponds to the global minimum on the PES[19, 20] and, accordingly, as shown by the calculations,[21] the crystal structure of supertetrahedral aluminum (Fig. 1) is dynamically stable.

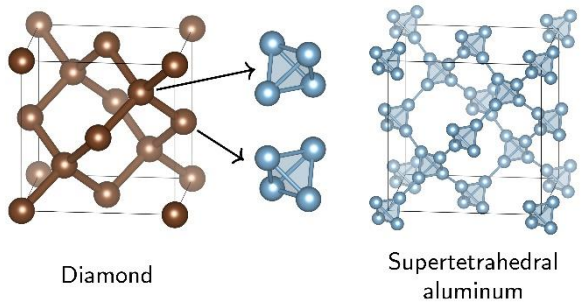


**Figure 1.** The conventional cubic unit cells of the crystal structure of diamond (left) and supertetrahedral aluminum (right). Atoms C and Al are designated by brown and blue colors, respectively.

The calculations performed within the framework of the density functional theory showed[21] that supertetrahedral aluminum is expected to be a very light material. Its density was calculated to be equal to as low as 0.61 g/cm$^3$, which is more than four times less than the density of the ordinary fcc aluminum and one and a half times less than the density of water. As well as the fcc aluminum, supertetrahedral aluminum is a conductor. However, after previous calculations, the question remained to be answered: at what temperatures the crystal structure of the supertetrahedral aluminum is kept on stable? One of the aims of the present study was to elucidate this issue using *ab initio* molecular dynamics modeling (AIMD) to determine the maximum temperature at which supertetrahedral aluminum retains its structural stability.

Equally important are the studies of the chemical bonding nature of aluminum and its allotropic modification. The theoretical and experimental studies of electron distribution in solid aluminum began in the 1920s[22]. These culminated[23] in the combined experimental and theoretical investigation of the bonding electron density at the aluminum in the terms of free electron gas and were continued in [24-26]. At the same time, the chemical bonding pattern of supertetrahedral aluminum was not previously deciphered in terms of multicenter chemical bonds and Adaptive Natural Density Partitioning (AdNDP) scheme[27,28]. Therefore, another goal of the present study was to gain insight into the chemical bonding pattern of supertetrahedral aluminum and its transformation during the phase transition processes.

## II. METHODS

The solid-state calculations were carried out using Vienna Ab initio Simulations Package (VASP)[29-32] with projector augmented wave (PAW) pseudopotentials[33,34] and the PBEsol[35] exchange-correlation functional. The $3s^2 3p^1$ electrons were treated as valence electrons for Al. For the plane wave expansion, we use a cut-off energy of 250 eV. The Brillouin zone was sampled by the Monkhorst-Pack method[36] with an automatic generated grid of 3×3×3 for

chemical bonding calculations, while the Molecular dynamics (MD) simulations employed gamma-point calculations due to the significant size of the supercell. The convergence criterion for total energies was $10^{-8}$ eV per atom. The MD simulations of homogeneous melting of crystal structures were performed at a constant number of particles, constant pressure of 1 bar, and constant temperature (*NpT* ensemble). The pressure and temperature in the simulation were controlled by Parrinello-Rahman barostat[37,38] and Langevin thermostat,[39] respectively. The computational supercell for fcc aluminum was obtained as 4×4×4 face-centered cubic unit cells involving 256 aluminum atoms. The computational supercell for supertetrahedral aluminum was obtained as 2×2×2 face-centered cubic unit cells involving 256 aluminum atoms. A time step of 4 fs was used for the integration of Newton's equations of motion. The initial positions of the atoms correspond to the relaxed fcc aluminum or supertetrahedral aluminum crystal structures. The initial velocities of the atoms are set randomly according to a Maxwell-Boltzmann distribution at the initial temperature. The crystal melting was detected by the change of the pair correlation function, which demonstrates the disappearance of long-range order in the arrangement of atoms in the case of a solid-to-liquid phase transition.

To analyze the chemical bonding pattern of the supertetrahedral aluminum and fcc aluminum, the solid-state adaptive natural density partitioning (SSAdNDP)[40] algorithm was used. SSAdNDP follows an idea of the periodic NBO method[41] and allowed us to obtain not only classical Lewis elements such as one-center two-electron (1c-2e) lone pairs and two-center two-electron (2c-2e) bonds but also delocalized bonding elements (*n*c-2e). A plane-wave calculation was performed using a 400 eV energy cutoff with a convergence threshold of $10^{-8}$ eV for the total energy. Then, plane-wave density was projected into the def2-TZVP[42] AO basis set. Previously, it was shown that the SSAdNDP is a powerful tool for analyzing chemical bonding in materials.[43-45] The face-centered cubic unit cells involving 32 aluminum atoms was chosen for the chemical bonding analysis of supertetrahedral aluminum. The chemical bonding pattern of a model cluster ($Al_4H_4$) was obtained using the AdNDP algorithm[27] as implemented in the AdNDP 2.0 code.[28] All calculations for the molecule were performed using the Gaussian 16 software[46] package at the PBE0/def2-TZVP level.[47,48]

The unit cells of crystal structures and obtained solid-state bonding patterns were visualized with VESTA software[49]. The MD simulation process was investigated and visualized using OVITO program[50]. The molecular chemical bonding pattern was visualized by the Chemcraft program[51].

## III. RESULTS AND DISCUSSION

At the beginning of our study, we investigated the structural stability of conventional fcc aluminum at various temperatures and carried out a series of molecular dynamics calculations at constant temperatures of 1500, 1400, 1300, and 1200 K. It was found that at 1500 K melting of fcc aluminum occurred after 3 ps (Fig. S1), at 1400 K – after 5 ps (Fig. S2), at 1300 – after 37 ps from the beginning of molecular dynamics simulation (Fig. 2). No melting was found by the AIMD

simulations performed at 1200 K for 195 ps (Fig. S3) and at 1250 K (Fig. 3) for 195 ps each (Fig. 3. It, therefore, may be concluded that the lowest temperature at which the process of homogeneous melting of ordinary fcc aluminum occurs lies in the range of 1250-1300 K. This temperature is 1.34-1.39 times higher than the melting temperature of ordinary (heterogeneous) aluminum (933 K)[52] which might be an indication that the AIMD simulation at chosen level of theory and a chosen time range slightly overestimates the melting point temperatures. Another reason for high melting point could be a different mechanism of melting, which cannot be described within the periodic boundary conditions.

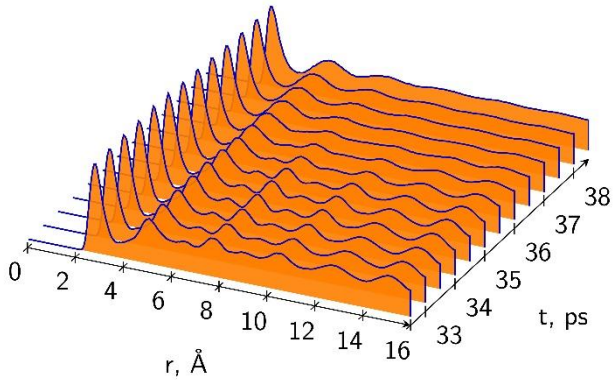


**Figure 2.** The pair-correlation function vs time of AIMD simulation for fcc aluminum obtained from simulation at a constant temperature of 1300 K. The graphs correspond to a time range of 32.5–38.5 ps with the 0.5 ps increment.

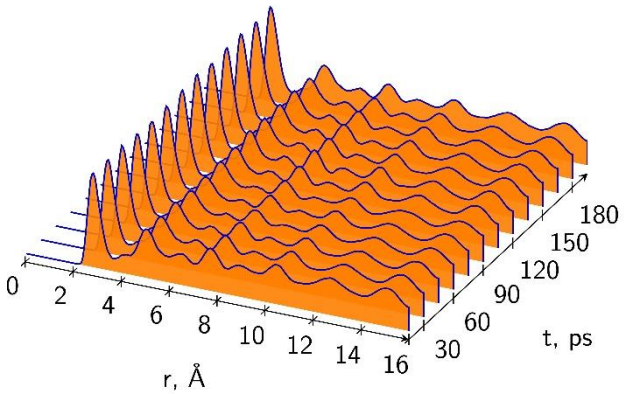


**Figure 3.** The pair-correlation function vs time of AIMD simulation for fcc aluminum obtained from simulation at a constant temperature of 1250 K. The graphs correspond to a time range of 15–195 ps with the 5 ps increment.

Next, we studied the structural stability of supertetrahedral aluminum at different temperatures. According to the AIMD simulation carried out at 800 K its crystal structure immediately collapses at these conditions and the system converts to a liquid state (Fig. S4). Then we ran a series of AIMD simulations gradually decreasing the temperature by 100 K from 700 to 300 K and found that in all the cases melting of supertetrahedral aluminum rapidly occurred. At temperatures of 700, 600 and 500 K, the melting process began immediately and ended 2-3 ps after the start of the simulation (Fig. S5-S7). At 400 K and 300 K, sample melting began

after 2-3 ps of the AIMD simulation (Fig. S8-S9). No melting occurs at 200 K for at least 325 ps from the start of the simulation (Fig. 4).

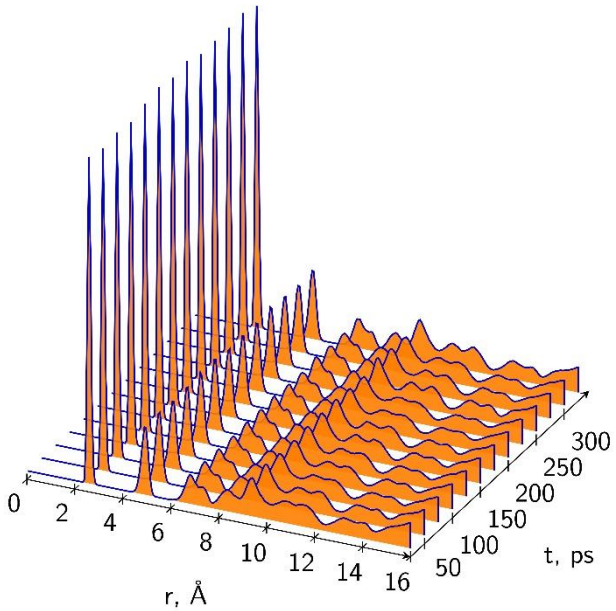


**Figure 4.** The pair-correlation function vs time of AIMD simulation for supertetrahedral aluminum obtained from the simulation at a constant temperature of 200 K. The graphs correspond to a time range of 25–325 ps with the 25 ps increment.

Based on the results of the performed AIMD simulations it can be concluded that at a temperature of 200 K supertetrahedral aluminum retains its crystal structure. The AIMD simulation performed at 250 K reveals that melting begins in 22 ps from the start of the simulation (Fig. S10). The simulation run at 225 K showed that melting began in 68 ps from the start of the simulation (Fig. 5). Thus, the statement made in the original publication that super tetrahedral aluminum would float in water was an overestimation, since the temperature of 200K is too low to keep water in liquid phase under ambient pressure.[21] However, the supertetrahedral aluminum can float in liquid nitrogen, since the boiling point of $N_2$ is 77K and the density is 0.81 g/cm$^3$ (which is greater than the density of supertetrahedral aluminum).[52] We note that, the computational modeling and DFT approximation could give us only an assessment of melting point, and the deviations from experimental values might be observed.

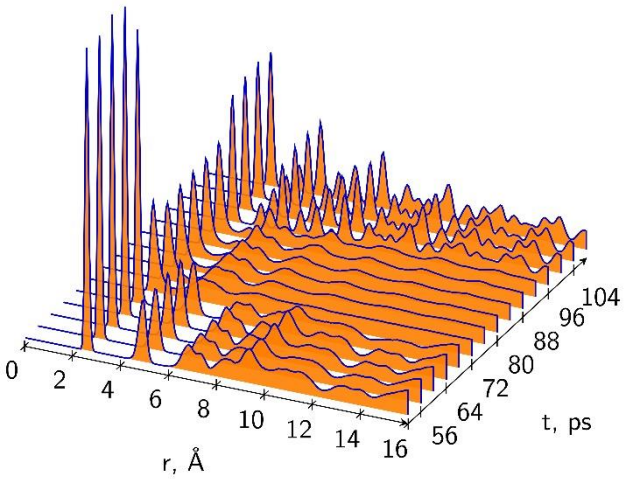


**Figure 5.** The pair-correlation function vs time of AIMD simulation for supertetrahedral aluminum obtained from the simulation at a constant temperature of 225 K. The graphs correspond to a time range of 52–108 ps with the 4 ps increment.

Interestingly, it was found, that at a temperature of 225 K phase transformations of supertetrahedral aluminum are not limited only to its melting. Our calculations show that the melting process begins with the shortening of distances between $Al_4$ tetrahedra. After that, the additional bonds between $Al_4$ tetrahedra begin to form and more complex conglomerates appears. Then, the process of atom rearrangements begins within these conglomerates with breaking of some bonds and formation of other bonds. Further, after 96 ps from the start of the AIMD simulation, a liquid-to-solid phase transition occurs (Fig. 5) with the formation of conventional crystalline aluminum with the fcc crystal structure. Figure 6 illustrates the cohesive energy per atom changes occurring during the process of molecular dynamics simulation at a constant temperature of 225 K. The transformation of supertetrahedral aluminum into ordinary fcc aluminum releases energy equal to 1.19 eV/atom (4260 kJ/kg).

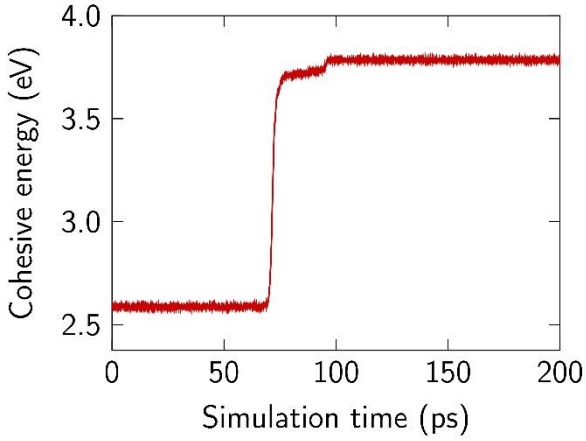


**Figure 6.** Cohesive energy per atom vs time of AIMD simulation for supertetrahedral aluminum according to the simulation at a constant temperature of 225 K.

We performed the calculations of phonon density of states (DOS) of supertetrahedral aluminum at 200 and 225 K *via* velocity autocorrelation functions from the AIMD simulations (Figure S11). The plots of the phonon DOS at 200 K и 225 K are almost identical to each other, which can be explained by the small difference between the temperature values of 200 and 225 K. At the same time, both graphics are very different from the phonon DOS at 0 K obtained in the original paper using the harmonic approximation.[21] This suggests that the oscillations of the ions in supertetrahedral aluminum at 200 and 225 K are essentially anharmonic.

To get insights into the chemical bonding of supertetrahedral aluminum we firstly analyzed the chemical bonding of the $Al_4H_4$ cluster as it is a unit fragment constituting the material of interest. The results of AdNDP analysis are shown in Figure 7. The chemical bonding of $Al_4H_4$ can be described as four classical 2c-2e Al-H σ-bonds with occupancy number (ON) of 2.00 |e| (Fig. 7B), and four 3c-2e σ-bonds with ON = 1.93 |e| (Fig. 7C) that provide bonding interaction within each $Al_3$ triangle. However, we should note that the found 3c-2e bonding elements have a large overlap with each other, and since the AdNDP procedure does not include orthogonalization of found bonding elements, the ONs of those bonds are overestimated. To calculate the true ON we localized each 3c-2e bonding element one by one, thus depleting the density matrix in a way that does not account for the same density twice. With the described procedure the ON of 3c-2e bonds is 1.75 |e|, and ~0.77 |e| is overcounted in the conventional AdNDP procedure. We note that NBO analysis (that produces orthogonal localized bonding elements) agrees with the corrected AdNDP occupancies of 3c-2e elements resulting in ONs = 1.75 |e|.

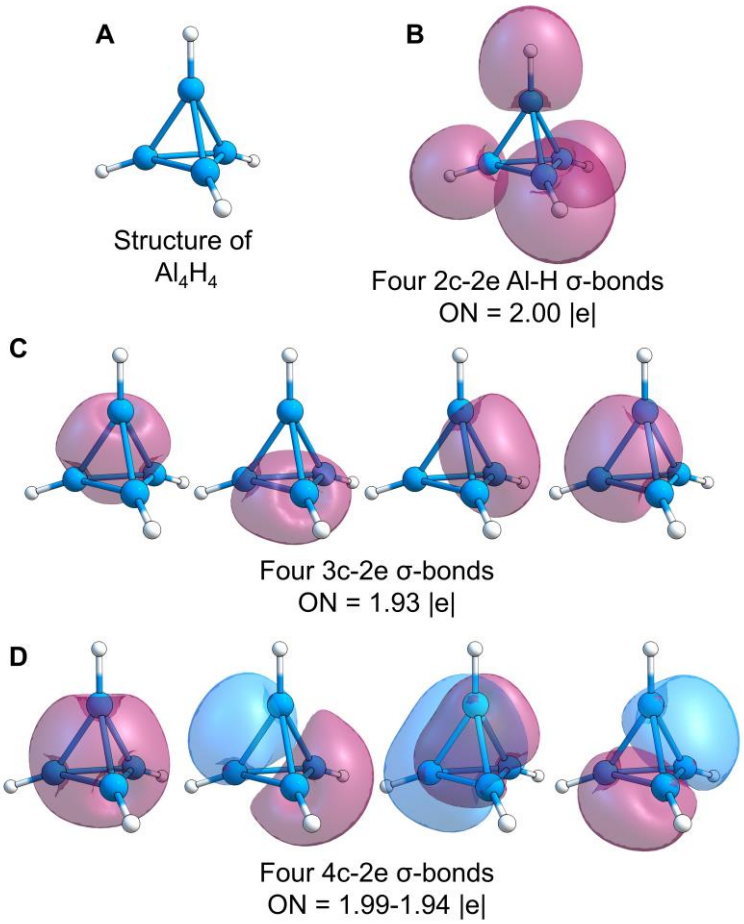


**Figure 7.** Chemical bonding pattern of $Al_4H_4$. (A) optimized structure of $Al_4H_4$; (B) 2c-2e Al-H σ-bonds; (C) possible partitioning into 3c-2e σ-bonds; (D) possible partitioning into 4c-2e σ-bonds.

Such an overestimation led us to the conclusion that the delocalization within $Al_4$ tetrahedron might be more properly described with 4c-2e bonding elements. Indeed, the AdNDP localized four 4c-2e σ-bonds (Fig. 7D) with high ON = 1.99–1.94 |e|. That solution does not suffer from the overestimation of electron density since each bonding element is localized accounting for the density of the previous element.

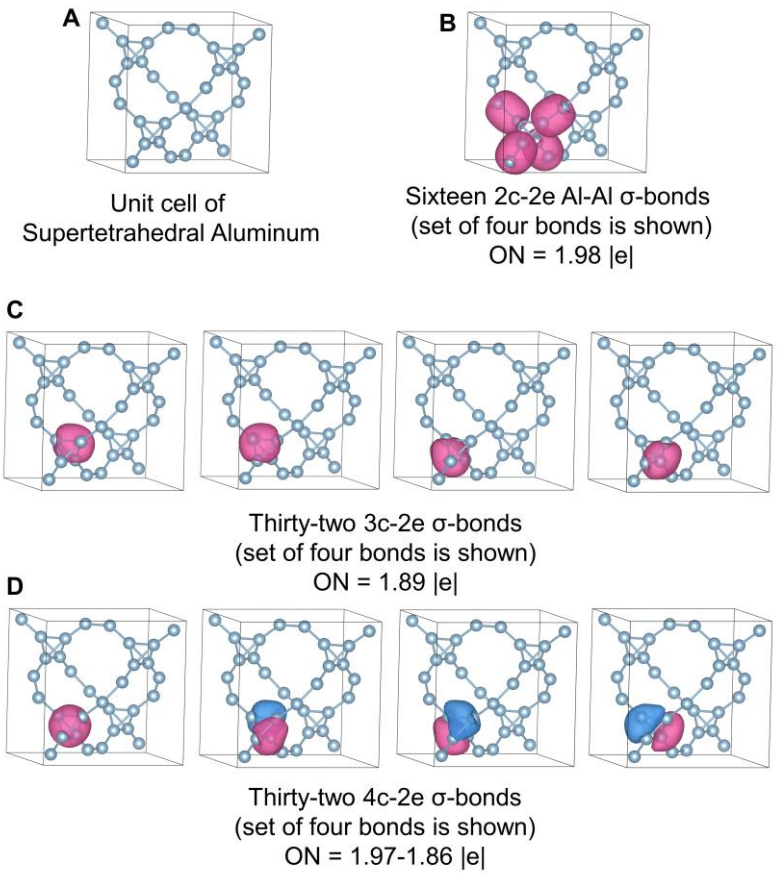


**Figure 8.** Chemical bonding pattern of supertetrahedral aluminum. (A) relaxed structure of unit cell; (B) 2c-2e Al-Al σ-bonds; (C) possible partitioning into 3c-2e σ-bonds; (D) possible partitioning into 4c-2e σ-bonds.

Following the insights obtained from the bonding of $Al_4H_4$ cluster, we analyzed the chemical bonding pattern of the supertetrahedral aluminum via SSAdNDP algorithm. The results are presented in Figure 8. Since 32 aluminum atoms are included into a unit cell, there are eight $Al_4$ tetrahedra involved. However, we found from SSAdNDP analysis, that the chemical bonding of all $Al_4$ is similar with each other, since every tetrahedra have the same surroundings. Thus, in Figure 8, the chemical bonding elements for a single tetrahedra are shown for clarity. Each $Al_4$ is bound to neighboring $Al_4$ fragments via four 2c-2e Al-Al σ-bonds with ON = 1.98 |e| (Fig. 8B). Similarly, to the $Al_4H_4$ case, the intra-cluster bonding can be described via 3c-2e σ-bonds with ON = 1.89 |e| (Fig. 8C). The significant overlap within 3c-2e σ-bonds is also present in the case of solid-state supertetrahedral aluminum, and the overestimation of the density is ~0.58 |e|. Using the same approach as was described in the case of $Al_4H_4$, the true ONs of 3c-2e σ-bonds was found to be 1.75 |e|. Alternatively, eight intra-cluster bonding electrons could be localized in four 4c-2e σ-bonds with high ON = 1.97–1.86 |e|. We note that the occupation numbers found in a supertetrahedral aluminum are lower than that found in the molecular system. The reason of this is the partial global delocalization of electron density associated with the conductive properties of the material.[43]

As was mentioned above, during the AIMD simulation the phase transition from supertetrahedral aluminum to fcc aluminum was observed. Thus, we also analyzed

the chemical bonding pattern of fcc Al,[53] to understand the evolution of chemical bonding after the phase transition. Due to the high degree of delocalization, the SSAdNDP could not localize any bonding elements from valence electrons with high ONs and proper symmetry within the unit cell. Thus, the chemical bonding of supertetrahedral aluminum transforms into a metallic bond after the phase transition.

## IV. CONCLUSIONS

The reported *ab initio* molecular dynamics simulations showed that supertetrahedral aluminum remains structurally stable at the temperatures of 200 K and below. At 225 K, in 68 ps from the start of the AIMD simulation, supertetrahedral aluminum melts, followed by a liquid-to-solid phase transition with the formation of conventional fcc aluminum. This transformation is accompanied by energy release of 4260 kJ/kg. Based on the temperature stability and the density of supertetrahedral aluminum, this material can float in liquid nitrogen. We found that the chemical bonding of supertetrahedral aluminum could be described via localized 2c-2e bonds between $Al_4$ units and four intra-cluster 3c-2e (or 4c-2e) bonding elements within one $Al_4$ unit. The transition from supertetrahedral form to the regular fcc structure accompanied with the formation of the metallic bonding without any localized bonding elements, which might be a reason of a significant energy release in phase transition process. We believe that the results obtained in this work strengthen the possibility of future fabrication of the supertetrahedral aluminum and in general will guide future research on ultralight materials.

## ASSOCIATED CONTENT

**Supporting Information.** The PDF file contains: Fig. S1-S3 (evolution with time of the pair-correlation function for fcc aluminum from molecular dynamics simulation at constant temperature of 1500, 1400 and 1200 K); Fig. S4-S10 (evolution with time of the pair-correlation function for supertetrahedral aluminum from molecular dynamics simulation at constant temperature of 800, 700, 600, 500, 400, 300 and 250 K); Table S1 (optimized geometry of the $Al_4H_4$ molecule); the video file contain the visualization of the molecular dynamics simulation of supertetrahedral aluminum at 225K.

## ACKNOWLEDGMENTS

The work was supported by the Russian Ministry of Science and Education of the Russian Federation (State assignment in the field of scientific activity, Southern Federal University, no. 0852-2020-0019). A.I.B. acknowledges financial support from the R. Gaurth Hansen Professorship fund. The support and resources from the Centre for High Performance Computing at the University of Utah are gratefully acknowledged.

## CONFLICT OF INTERESTS

The authors declare that there is no conflict of interest.

## DATA AVAILABILITY

Additional data that support the findings of this study are available from the corresponding authors on a request.

## REFERENCES


[1] A. Gupta, T. Sakthivel, S. Seal, S. *Prog. Mater. Sci.* **2015**, *73*, 44-126.
[2] Z. Li, Z. Liu, H. Sun, C. Ga, *Chem. Rev.* **2015**, *115*, 7046-7117.
[2] N. Karousis, I. Suarez-Martinez, C. P. Ewels, N. Tagmatarchis, *Chem. Rev.* **2016**, *116*, 4850-4883.
[4] Z. Lin, *Acc. Chem. Res.* **2010**, *43*, 602-611.
[5] M. D. Ben, J. Hutter, J. VandeVondele, *J. Chem. Theory Comput.* **2012**, *8*, 4177-4188.
[6] K. S. Kim, Y. Zhao, H. Jang, S. Y. Lee, J. M. Kim, K. S. Kim, J.-H. Ahn, P. Kim, J.-Y. Choi, B. H. Hong, *Nature* **2009**, *457*, 706-710.
[7] A. Reina, X. Jia, J. Ho, D. Nezich, H. Son, V. Bulovic, M. S. Dresselhaus, J. Kong, *Nano Lett.* **2009**, *9*, 30-35.
[8] P. Vogt, P. De Padova, C. Quaresima, J. Avila, E. Frantzeskakis, M. C. Asensio, A. Resta, B. Ealet, G. Le Lay, *Phys. Rev. Lett.* **2012**, *108*, 155501(5).
[9] V. Georgakilas, J. A. Perman, J. Tucek, R. Zboril, *Chem. Rev.* **2015**, *115*, 4744-4822.
[10] R. B. Heimann, S. E. Evsvukov, Y. Koga, *Carbon* **1997**, *35*, 1654-1658.
[11] P. Jena, Q. Sun, *Chem. Rev.* **2018**, *118*, 5755-5870.
[12] N. V. Tkachenko, D. Steglenko, N. Fedik, N. M. Boldyreva, R. M. Minyaev, and V. I. Minkin, A. I. Boldyrev, *Phys. Chem. Chem. Phys.* **2019**, *21*, 19764-19771.
[13] D. V. Steglenko, N. V. Tkachenko, A. I. Boldyrev, R. M. Minyaev, and V. I. Minkin, *J. Comput. Chem.* **2020**, *41*, 1456–1463.
[14] J. K. Burdett, S. Lee, *J. Am. Chem. Soc.* **1985**, *107*, 3063-3082.
[15] R. J. Johnston, R. Hoffmann, *J. Am. Chem. Soc.* **1989**, *111*, 810-819.
[16] P. Miró, M. Audiffred, T. Heine, *Chem. Soc. Rev.* **2014**, *43*, 6537-6554.
[17] J. Neugebauer, T. Hickel, *WIREs Comput. Mol. Sci.* **2013**, *3*, 438-448.
[18] I. V. Getmanskii, R. M. Minyaev, D. V. Steglenko, V. V. Koval, S. A. Zaitsev, V. I. Minkin, *Angew. Chem. Int. Ed.* **2017**, *56*, 10118-10122.
[19] R. Haunschild, G. Frenking, *Mol. Phys.* **2009**, *107*, 911-922.
[20] R. M. Minyaev, I. A. Popov, V. V. Koval, Alexander I. Boldyrev, Vladimir I. Minkin, *Struct Chem* **2015**, *26*, 223–229.
[21] I. V. Getmanskii, V. V. Koval, R. V. Minyaev, A. I. Boldyrev, V. I. Minkin, *J. Phys. Chem. C* **2017**, *121*, 22187-22190.
[22] J. A. Bearden, *Phys. Rev*. **1927**, *29*, 20-33.
[23] P. N. H. Nakashima, A. E. Smith, J. Etheridge, B. C. Muddle, *Science* **2011**, *331*, 1583-1586.
[24] P. N. H. Nakashima, *Struct. Chem.* **2017**, *28*, 1319–1332.

[25] P. N. H. Nakashima in *Encyclopedia of Aluminum and Its Alloys* (Eds.: G. E. Totten, M. Tiryakioğlu, O. Kessler), Boca Raton: CRC Press, **2018**, 488–586.
[26] T. Sasaki, H. Kasai, E. Nishibori, *Sci. Rep.* **2018**, *8*, 11964.
[27] D. Yu. Zubarev, A. I. Boldyrev, *Phys. Chem. Chem. Phys.* **2008**, *10*, 5207–5217.
[28] N. V. Tkachenko, A. I. Boldyrev, *Phys. Chem. Chem. Phys.* **2019**, *21*, 9590-9596.
[29] G. Kresse, J. Hafner, *Phys. Rev. B: Condens. Matter Mater. Phys.* **1993**, *47*, 558-561.
[30] G. Kresse, J. Hafner, *Phys. Rev. B: Condens. Matter Mater. Phys.* **1994**, *49*, 14251-14269.
[31] G. Kresse, J. Furthmüller, *Phys. Rev. B: Condens. Matter Mater. Phys.* **1996**, *54*, 11169-11186.
[32] G. Kresse, J. Furthmüller, *Comput. Mater. Sci.* **1996**, *6*, 15-50.
[33] P. E. Blöchl, *Phys. Rev. B: Condens. Matter Mater. Phys.* **1994**, *50*, 17953-17979.
[34] G. Kresse, D. Joubert, *Phys. Rev. B: Condens. Matter Mater. Phys.* **1999**, *59*, 1758-1775.
[35] J. P. Perdew, A. Ruzsinszky, G. I. Csonka, O. A. Vydrov, G. E. Scuseria, L. A. Constantin, X. Zhou, K. Burke, *Phys. Rev. Lett.* **2008**, **100**, 136406.
[36] Monkhorst, H. J.; Pack, J. D. Special Points for Brillouin-Zone Integrations. *Phys. Rev. B: Condens. Matter Mater. Phys.* **1976**, *13*, 5188-5192.
[37] M. Parrinello, A. Rahman, *Phys. Rev. Lett.* **1980**, *45*, 1196-1199.
[38] A. Rahman, M. Parrinello, *J. Appl. Phys.* **1981**, *52*, 7182-7190.
[39] M. P. Allen, D. J. Tildesley, *Computer Simulation of Liquids*; Oxford University Press: New York, **1991**.
[40] T. R. Galeev, B. D. Dunnington, J. R. Schmidt, and A. I. Boldyrev, *Phys. Chem. Chem. Phys.* **2013**, *15* , 5022
[41] B. D. Dunnington, and J. R. Schmidt, *J. Chem. Theory Comput.* **2012**, *8*, 1902.
[42] Weigend, F., and Ahlrichs, R. *Phys. Chem. Chem. Phys.* **2005**, *7*, 3297–3305.
[43] Rublev P., Tkachenko N. V., and Boldyrev A. I., *J. Comput. Chem.* **2022**, DOI: 10.1002/jcc.26854.
[44] Kulichenko M., and Boldyrev A. I., *J. Phys. Chem. C*, **2020**, *124*, 6267-6273.
[45] Tkachenko N. V., Song B., Steglenko D., Minyaev R. M., Yang L.-M., and Boldyrev A. I., *Phys. Status Solidi B*, **2020**, *257*, 1900619.
[46] Gaussian 16, Revision C.01, M. J. Frisch, G. W. Trucks, H. B. Schlegel, G. E. Scuseria, M. A. Robb, J. R. Cheeseman, G. Scalmani, V. Barone, G. A. Petersson, H. Nakatsuji, X. Li, M. Caricato, A. V. Marenich, J. Bloino, B. G. Janesko, R. Gomperts, B. Mennucci, H. P. Hratchian, J. V. Ortiz, A. F. Izmaylov, J. L. Sonnenberg, D. Williams-Young, F. Ding, F. Lipparini, F. Egidi, J. Goings, B. Peng, A. Petrone, T. Henderson, D. Ranasinghe, V. G. Zakrzewski, J. Gao, N. Rega, G. Zheng, W. Liang, M. Hada, M. Ehara, K. Toyota, R. Fukuda, J. Hasegawa, M. Ishida, T. Nakajima, Y. Honda, O. Kitao, H. Nakai, T. Vreven, K. Throssell, J. A. Montgomery, Jr., J. E. Peralta, F. Ogliaro, M. J. Bearpark, J. J. Heyd, E. N. Brothers, K. N. Kudin, V. N.

Staroverov, T. A. Keith, R. Kobayashi, J. Normand, K. Raghavachari, A. P. Rendell, J. C. Burant, S. S. Iyengar, J. Tomasi, M. Cossi, J. M. Millam, M. Klene, C. Adamo, R. Cammi, J. W. Ochterski, R. L. Martin, K. Morokuma, O. Farkas, J. B. Foresman, and D. J. Fox, Gaussian, Inc., Wallingford CT, **2016**.
[47] J. P. Perdew, K. Burke, M. Ernzerhof, *Phys. Rev. Lett.*, **1996**, *77*, 3865-3868.
[48] J. P. Perdew, K. Burke, M. Ernzerhof, *Phys. Rev. Lett.*, **1997**, *78*, 1396.
[49] M. Momma, F. Izumi, *J. Appl. Crystallogr.* **2011**, *44*, 1272-1276.
[50] A. Stukowski, *Model. Simul. Mater. Sci. Eng.* **2010**, *18*, 015012.
[51] G. A. Zhurko, Chemcraft - graphical program for visualization of quantum chemistry computations. Ivanovo, Russia, **2005**. https://chemcraftprog.com
[52] CRC Handbook of Chemistry and Physics, 84th ed.; Lide, D.R., Ed.; CRC Press: Boca Raton, FL, 2003;
[53] R. W. G. Wyckoff in *Crystal Structures. Second Edition*, Vol. 1, Interscience Publishers, New York, **1963**, pp. 7–83.